

## Performance Test of HCHB01

J. DiMarco, A. Hemmati, M.J. Kim, D. F. Orris, T. Page, R. Rabehl, M. Tartaglia, J.C. Tompkins

### Introduction

HCHB01 is the first Type-2 production cryostatted lens for the CH section of the HINS R&D proton linac. Previously a Type-1 prototype cryostat assembly HCH-P-001 was built and tested [1]. The cryostat design [2] for Type-2 lenses has 6 vapor-cooled current leads rated for 300 A operation (from Cryomagnetics, Inc.). These were positioned somewhat higher than the single pair of vapor-cooled leads in the prototype, to ensure that the superconductor splices are always in liquid helium. A photo of the assembly prior to completion of N<sub>2</sub> thermal shields and insulation and vacuum vessel walls is shown in Figure 1.

The production CH solenoid, HINS\_CH\_SOL\_T2\_01 (serial number 1201) was chosen for installation into the HCHB01 assembly. The solenoid in its liquid helium vessel was previously tested twice: first by the vendor (Cryomagnetics, Inc.) in 4.2 K helium at 1 atmosphere, and then again in a qualification test at 4.435 K in MTF stand 3: this solenoid then re-trained to its quench plateau in three quenches, and the steering dipole coils did not quench up to 250 A in the solenoid operating field at 180 A.

A production test plan for the assembled lenses follows the plan used to qualify individual cold masses, and adds elements to evaluate the thermal performance of the cryostat and of the lens as an optical system. In this note we report on the first execution of this plan, with results on quench training and ramp rate dependence of the solenoid, quench performance of the dipole coils, thermal properties of the cryostat, operating experience with the vapor-cooled current leads, and alignment studies on the solenoid and steering dipoles. A first pass on these measurements was made in two thermal cycles from room temperature to 4.5 K and back. After completing these tests, we found some interesting and unexplained results that need further investigation. Also, some additional tests are needed to optimize the operating parameters for the vapor-cooled leads. Therefore a supplemental test plan has been prepared and will be executed prior to testing of the first production Type-1 assembly, which is nearing completion.

### Solenoid Quench Performance

For accurate measurements of the solenoid temperature (and to ensure that it is in liquid helium), two calibrated Cernox sensors were installed during lens assembly, in the supply pipes just above the helium vessel. These correlate closely with the stand 6 feedbox sensors in saturated single phase helium. Cryogenic conditions in the cryostat on MTF stand 6 are somewhat warmer than in the earlier (vendor and stand 3) tests, and the ability to adjust the temperature is limited. Attempts to sub-cool the single phase helium were made, unsuccessfully, and these will be discussed later in the section on cryogenic performance. So, a temperature range from 4.50 to 4.65 K was achieved in this test.

During the first round of quench training studies, from 5/27-6/2/2010, the solenoid current lead flows were raised to a fairly high level, above 0.04 g/s each, to avoid any problems with lead-induced quenches. However, the dipole corrector leads were kept at a rather low flow of 0.01 g/s each. In all of the training studies, there was no evidence of anomalous (high) copper lead voltages, only coil voltage development was observed. Note that superconducting (SC) lead voltages are not monitored in this production device, following prototype studies that showed them to be unnecessary for SC lead quench protection [3].



Fig. 1. Photo of HCHB01 with internal assembly completed.

Solenoid quench performance was studied first at the nominal 1 A/s ramp rate for comparison to bare solenoid test data. The solenoid reached a plateau without any retraining quenches at 4.62 K. Subsequently, dependence of the quench current on temperature and ramp rate was explored. For the production cold mass qualification tests, ramp rate dependence was not studied, but it was with other R&D solenoids and the prototype cryostat assembly, HCH-P-001 [1]. Figure 2 shows that the ramp rate dependence for HCHB01 is much steeper than had been seen in R&D solenoids HINS\_CH\_SOL\_03d-1 [4] and HINS\_CH\_SOL\_06 [5], which showed the same or even slightly higher quench current up to 4 A/s. Still, it is not known if this greater sensitivity is related to the cryostat or is intrinsic to the solenoid. The turn-over at low ramp rate was curious, so some investigation into this was made. For reasons unknown (and still to be investigated) at ramp rates below 3 A/s, regulation of the power supply is not steady. This can be seen in Fig. 3 for the lowest ramp rate tried: while the average  $dI/dt$  is 0.22 A/s, the peak ramp rate is about 1.5 A/s. The red points in Fig. 1 indicate the trend versus peak ramp rate, rather than the average.

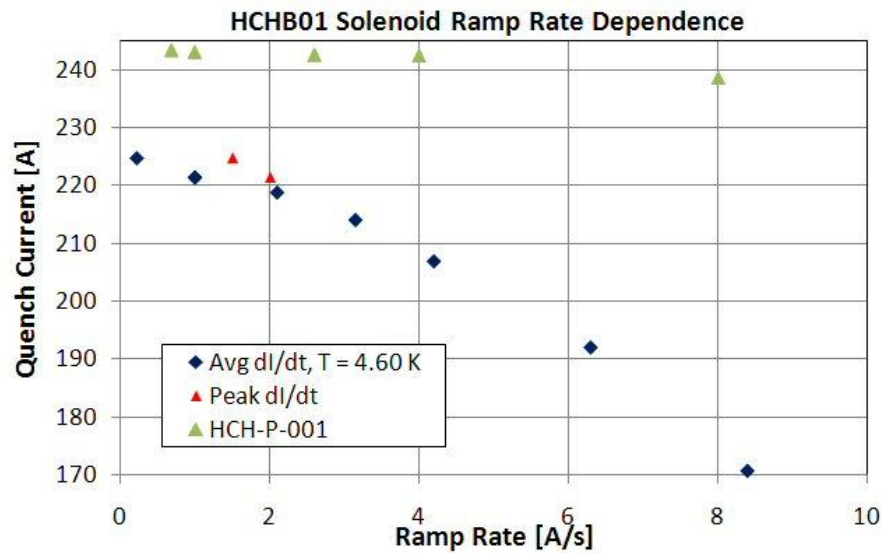


Fig. 2. Ramp rate dependence of quench current of the cryostatted solenoid at 4.60 K.

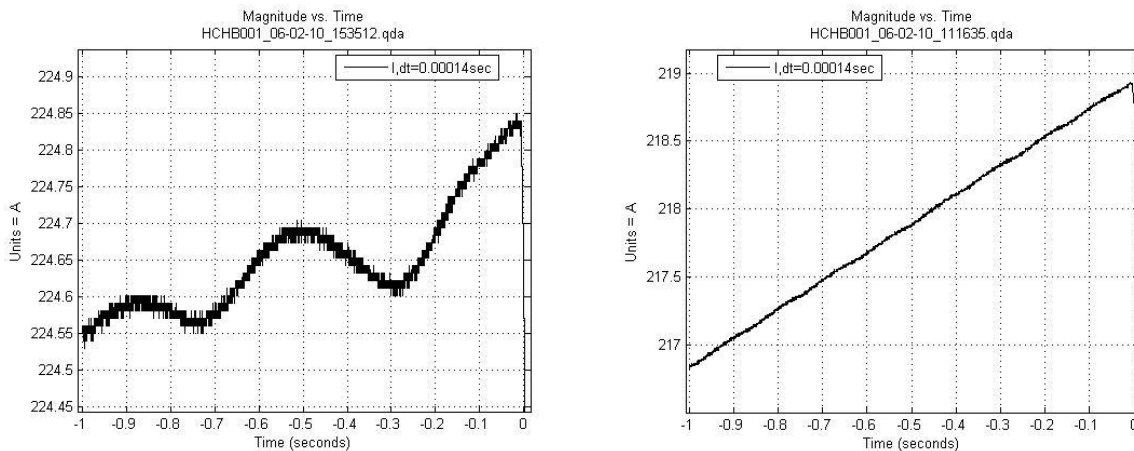


Fig. 3. Current rate of change, at 0.22 A/s (left) and 2 A/s (right) average ramp rate, just prior to quench.

Temperature dependence of the Type-2 solenoid quench current is summarized in Fig. 4. Vendor data at “4.2 K” (the precise temperature is not known, but tests were in boiling helium at atmospheric pressure) are shown for those magnets that appeared to have been fully trained; MTF data are shown for the re-tested solenoids (except T2\_09, which did not reach its expected maximum current and behaved somewhat erratically). The predicted temperature dependence trend for NbTi is shown as “model prediction”. The HCHB01 quench data at the “requested” 1 A/s ramp rate are plotted, with the 0.22 A/s data point added (filled red diamond) to illustrate the ramp rate effect. Finally, the trend for the prototype cryostat HCH-P-001 (and prototype solenoid CH\_SOL\_01-1 that was tested at 4.2 K) is scaled to match the T2\_01 behavior at 4.2 K.

Therefore, one can see that the quench performance of the cryostatted solenoid is below expectations, so the available operating margin is reduced. Previous data were taken with essentially the same ramp rate as for the production lens, so the actual quench current at 4.6 K is down at least 5 or perhaps 10 A, or about 3% low. Combined with the steep ramp rate dependence, this suggests something in the assembly or its operating regime may have caused a change in the solenoid behavior.

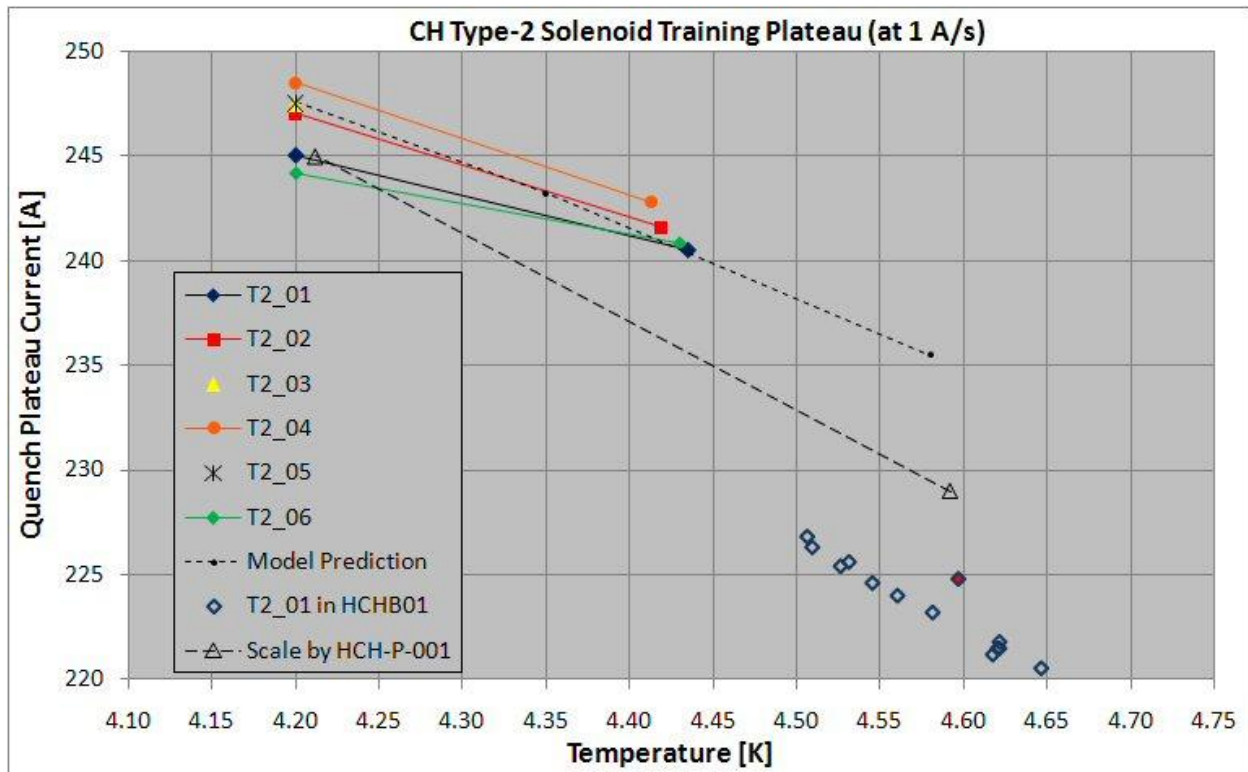


Fig. 4. Quench current versus helium bath temperature for Type-2 solenoids.

Dipole Quench Performance

As was done for all the Type-2 production cold masses, the steering dipoles were tested by ramping them to 250 A while holding the main solenoid at the nominal operating current of 180 A, with the expectation that they would not quench. This test was performed successfully at 4.60 K, and the history of actual currents recorded during the test is shown in Fig. 5.

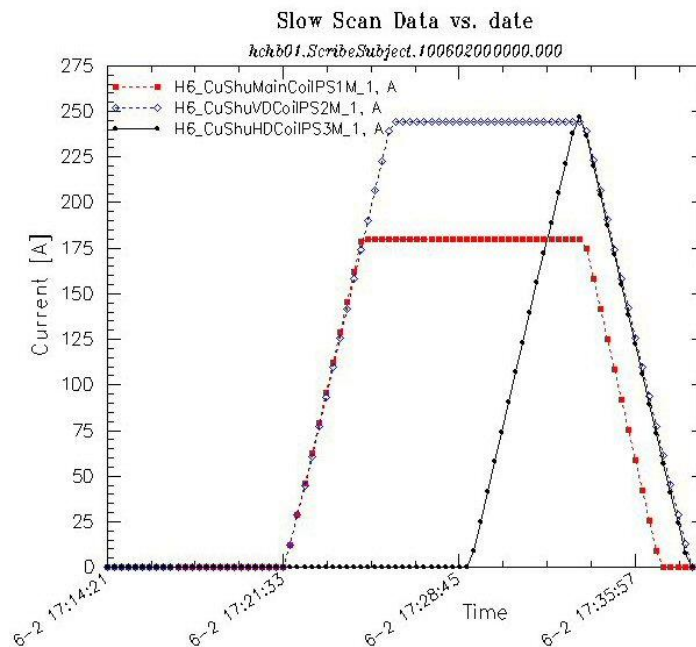


Fig. 5. Current history during (non-) quench performance test of steering dipoles.

### Cryostat Thermal Shield Performance

The first cool down of HCHB01 began on May 18, 2010 with flow of liquid N<sub>2</sub> to cool the shields and the N<sub>2</sub> control valve set to full open. The shield temperatures reached equilibrium within about 2 hours, at which point oscillations in temperature and pressure began to occur. Similar oscillations were evident in data from the prototype, HCH-P-001, which went away when liquid helium was flowed through that magnet. The HCHB01 N<sub>2</sub> flow was slowly reduced to find the minimum required flow to keep the shields cold (shields include the stand 6 feedbox, as well as the HINS cryostat – note that there is no shield in the interface between them): a minimum flow of 0.90 g/s nitrogen was required. Oscillations occurred at all flows above this value, and did not occur below it. These oscillations still occur intermittently following the cool down with helium.

These oscillations could be a result of two-phase flow into the warm-up coils mounted under the test stand. These are simply copper coils wound and plumbed on a horizontal axis. At high flow rates, LN<sub>2</sub> reaches these coils and accumulates. The result is slugging and unsteady flow. At low flow rates, LN<sub>2</sub> does not reach these coils. The flow is gas only and steady. The nature of the relationship between LHe flow and LN<sub>2</sub> behavior is not understood; although there is some thermal communication between these circuits, it should not be much.

The solenoid base shield temperature is measured with two platinum sensors, located as shown in Fig. 6. The liquid N<sub>2</sub> supply temperature in MTF is about 90 to 91K, at a pressure of about 45 psia. The stand 6 shields are typically operated with a nitrogen flow of about 2.5 g/s. Under these conditions the base shield temperatures were about 94 K, as shown in Fig. 7.

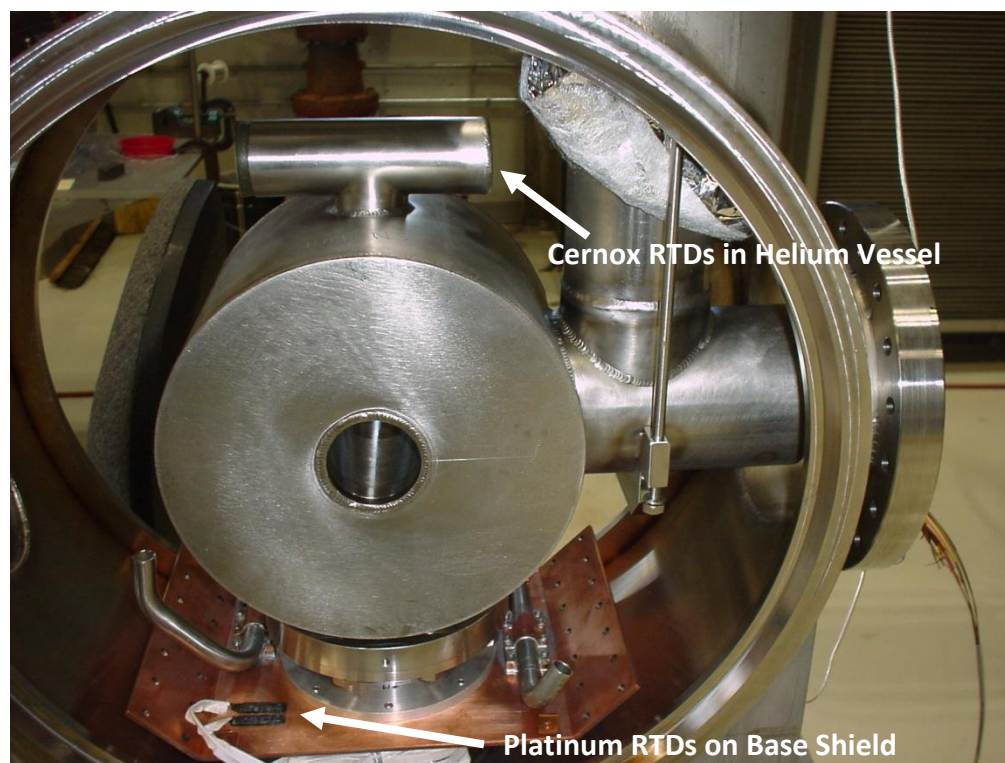


Fig. 6. Photograph of the cryostat during assembly, with RTD locations indicated.

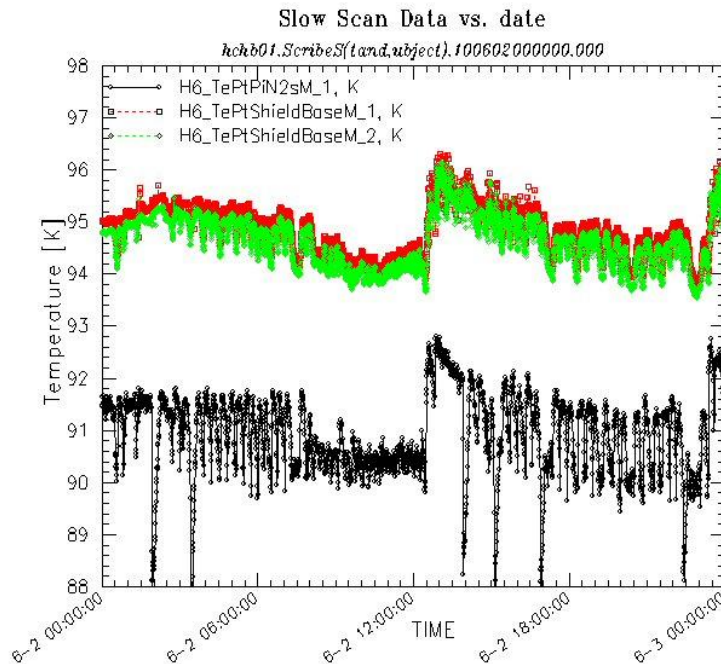


Fig. 7. Nitrogen supply and solenoid base shield temperatures; note intermittent oscillations.

### Helium System Performance

For the prototype HCH-P-001, two Cernox<sup>®</sup> temperature sensors were located in the helium vessel extension where splices to the superconducting power leads were made; in the production assembly, these were moved to the pipe above the solenoid (see Fig. 6), to indicate when the solenoid vessel is full of liquid. Fathom (model GR-112) 30 sl/m (standard liter per minute) flow sensors were installed to measure lead flow through each of the Cryomagnetics 300 Ampere vapor-cooled current leads; these sensors were calibrated for helium in October 2008, and monitored the mass flow rates of warm helium going back to the refrigeration plant compressor (one flow sensor, VD Positive Lead, did not work). The voltage across each current lead was also monitored by the scan system. As with HCH-P-001, each helium lead flow was controlled using a rota-meter with full range calibrated for 0-40 scfh (standard cubic feet per hour) of air. During the cold test, a cross check was made of the flow sensor reading as a function of the rota-meter setting, to estimate the level of error in flow adjustment, and check consistency of the device readouts. These data are plotted in Fig. 8.

The first helium cool down took place on 5/22, and quench performance testing began on 5/27 after completion of the cold electrical and protection system checkouts. During the quench performance testing, attempts were made to reach lower temperatures – to connect with stand 3 test data which were at about 4.4 K. These were not successful: even though the single phase input temperature at the feed box was sub-cooled to 4.3 K, the magnet temperature remained 4.6 K. This can be understood by studying the flow schematic for the test stand, shown in Fig. 9. The reason is that the solenoid helium vessel is below the supply pipe and acts like a dead

volume that does not mix well with the supply; so, in the cryogenic header sub-cooled liquid comes in, turns around at the return end and goes out through the JT valve, but does not cool the solenoid effectively.

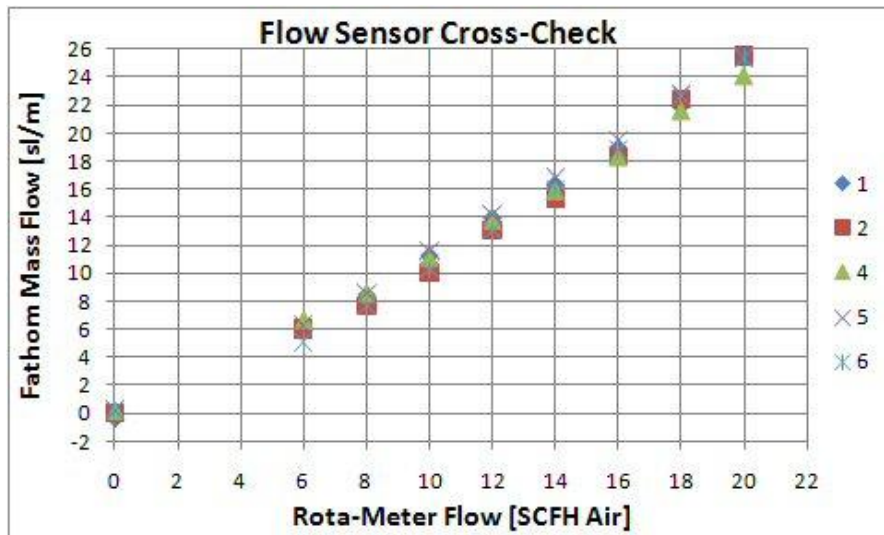


Fig. 8. Flow sensor reading versus Rota-meter set point.

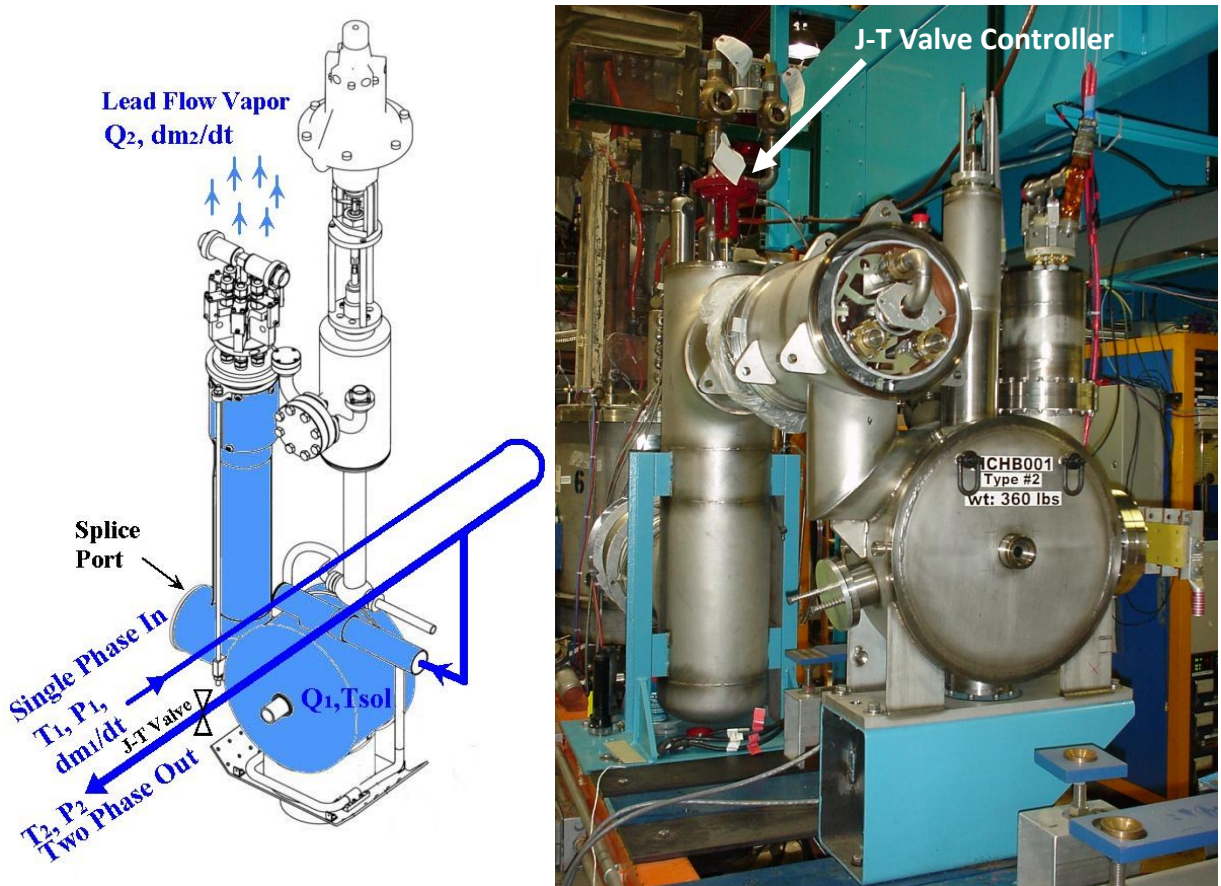


Fig. 9. Flow schematic for helium (blue) in the Type-2 CH lens in MTF (left); photo of the assembly return end during installation on the test stand (right).

The heat load to the helium system is an important parameter, especially for a beam line with many devices. Lacking a measure of the helium liquid level in the vessel, a simple boil-off rate test could not yield the answer. Instead, an experiment was set up to determine the heat load using energy balance in the system: the incoming single phase helium supply was sub-cooled at the feed box, and the J-T valve was fully opened so that the outgoing helium would also be single phase, sub-cooled liquid. By measuring the helium pressures (to verify sub-cooled conditions), the temperature rise and the total lead flow after reaching equilibrium, the heat input could be determined. Two tests were made: data taken on June 17 had constant lead flow conditions throughout, while data taken on July 9 were taken for a range of lead flow settings.

The heat balance is defined by Eqn. 1 where the cryogenic parameters are indicated in Fig. 9, and  $h$  is the enthalpy at the measured pressure and temperature of the sub-cooled liquid and  $h_v$  is the enthalpy of saturated vapor at the measured cryostat temperature. The results are shown in Fig. 10, heat load as a function of lead flow rate. Note that the nominal standby lead flow for three pair of these leads is estimated to be about 0.05 g/s. The calculated value for the cryostat is about 5 W, while the interface box estimate is about 9.3 W, which accounts for only about half of the measured 25 W heat load,  $Q_{total}$ . A reconfiguration of the test stand to measure the background heat load due to the feed box, return can, and interface box is planned, so that the heat load to the helium vessel within the cryostat can be accurately determined. Also, further study at lower lead flow rates would be useful to establish the standby minimum required flow.

$$Q_{Total} = \left( \frac{dm_1}{dt} - \frac{dm_2}{dt} \right) h_{\text{sub-cooled}}(P_2, T_2) - \frac{dm_1}{dt} h_{\text{sub-cooled}}(P_1, T_1) + \frac{dm_2}{dt} h_v(P_{sol}) \quad (1)$$

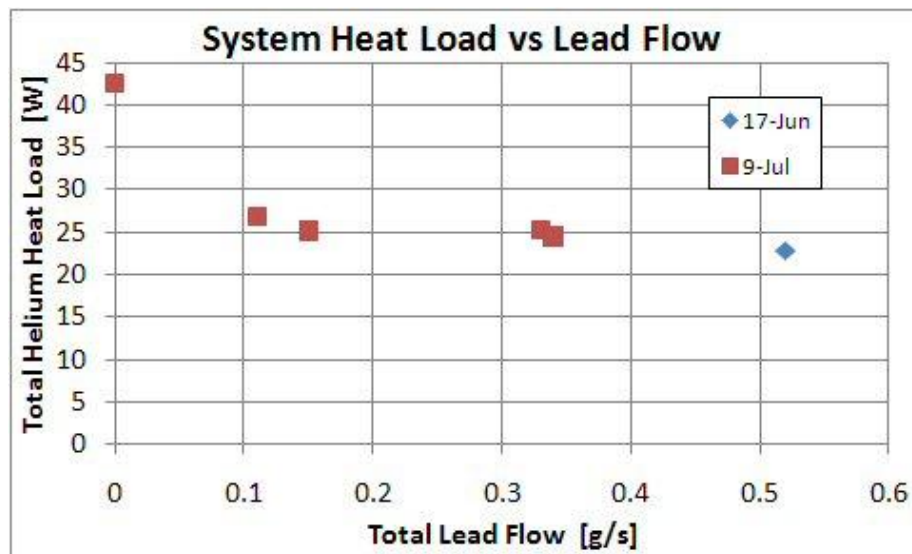


Fig. 10. Total heat load to the test stand plus solenoid lens helium system, versus total lead flow.

### Current Lead Performance

A study of the minimum required lead flow at the 180 A operating current was made on July 7. For this test, all of the lead flows were initially set to high values (0.05 g/s) and the solenoid current was ramped at 1 A/s to the 180 A operating plateau. The copper lead voltages were then monitored as the lead flow was stepped down toward zero, first for the positive lead and then for the negative lead. A graph of the lead flows, and solenoid current and lead voltages is shown in Fig. 11. When the positive lead flow was set at zero, the dipole corrector lead flows were also lowered (since they would not be powered, and frost was building up around the leads). The solenoid ran for 10 minutes with stable flows and no quench, and it can be seen that the positive lead voltage went up in response to lowering the other flows. With the positive lead flow at zero, the negative lead flow was then also stepped down to zero; at this point the positive flow was raised again to 0.016 g/s and voltages across both leads again responded. Note at 0.016 g/s the large difference in positive lead voltage, with the negative lead flow first at 0.05 g/s, and later at 0.0 g/s.

The inability to induce a quench at zero lead flow was a surprise, since this was easily done in the prototype HCH-P-001 above 90 A [3]. Clearly there is some mechanism for the lead temperatures to depend upon flows through the other leads, as well as their own.

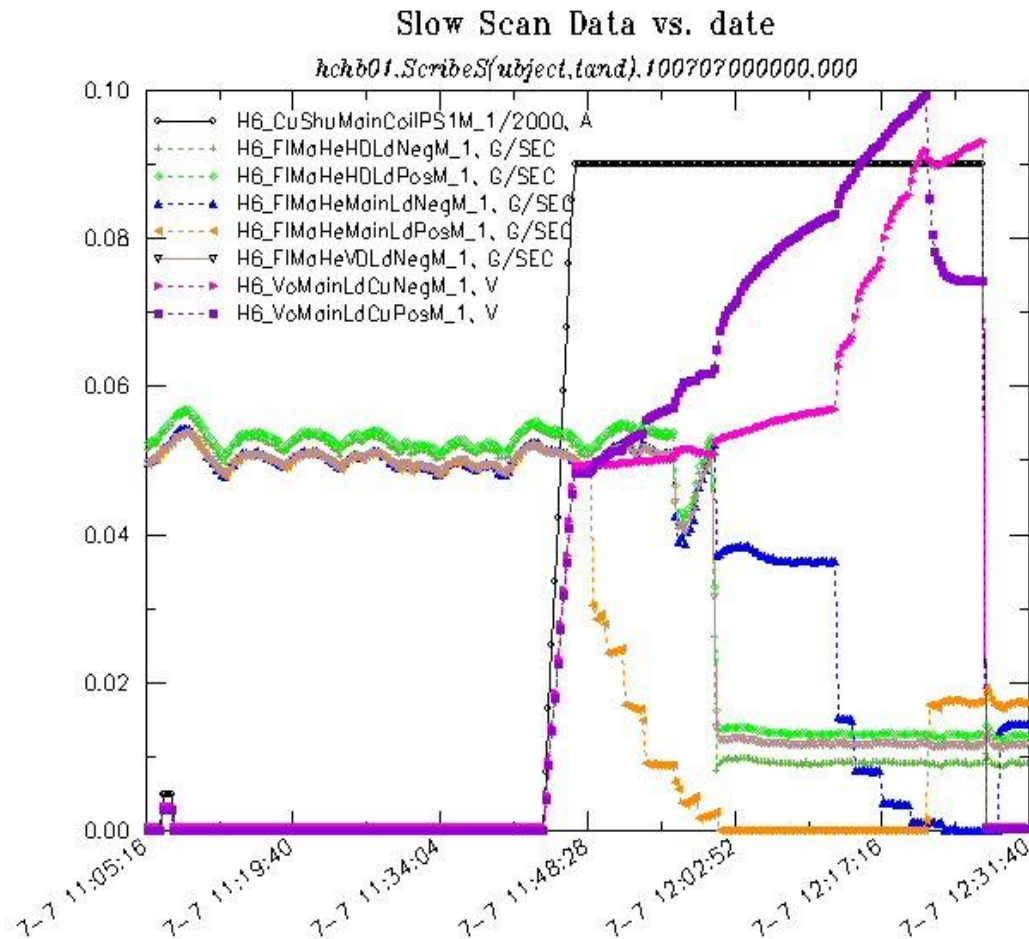


Fig. 11. Lead flows, solenoid current, and lead voltages versus time in minimum lead flow study.

This minimum flow study was continued on July 8, in which all leads were set to the same flow conditions using the Fathom readout as a guide (and the rota-meter for VD pos). Figure 12 shows the lead flow, solenoid current, and lead voltage history for this day, and a magnified view of the lead flows is shown in Fig. 13. The first setting was zero flow in all 6 leads, to see if any helium temperature rise could be detected by the thermometry in the feed box or solenoid vessel; the temperatures remained very steady. Flows were then raised in steps to 4 sl/m (0.012 g/s), and again temperatures remained unchanged.

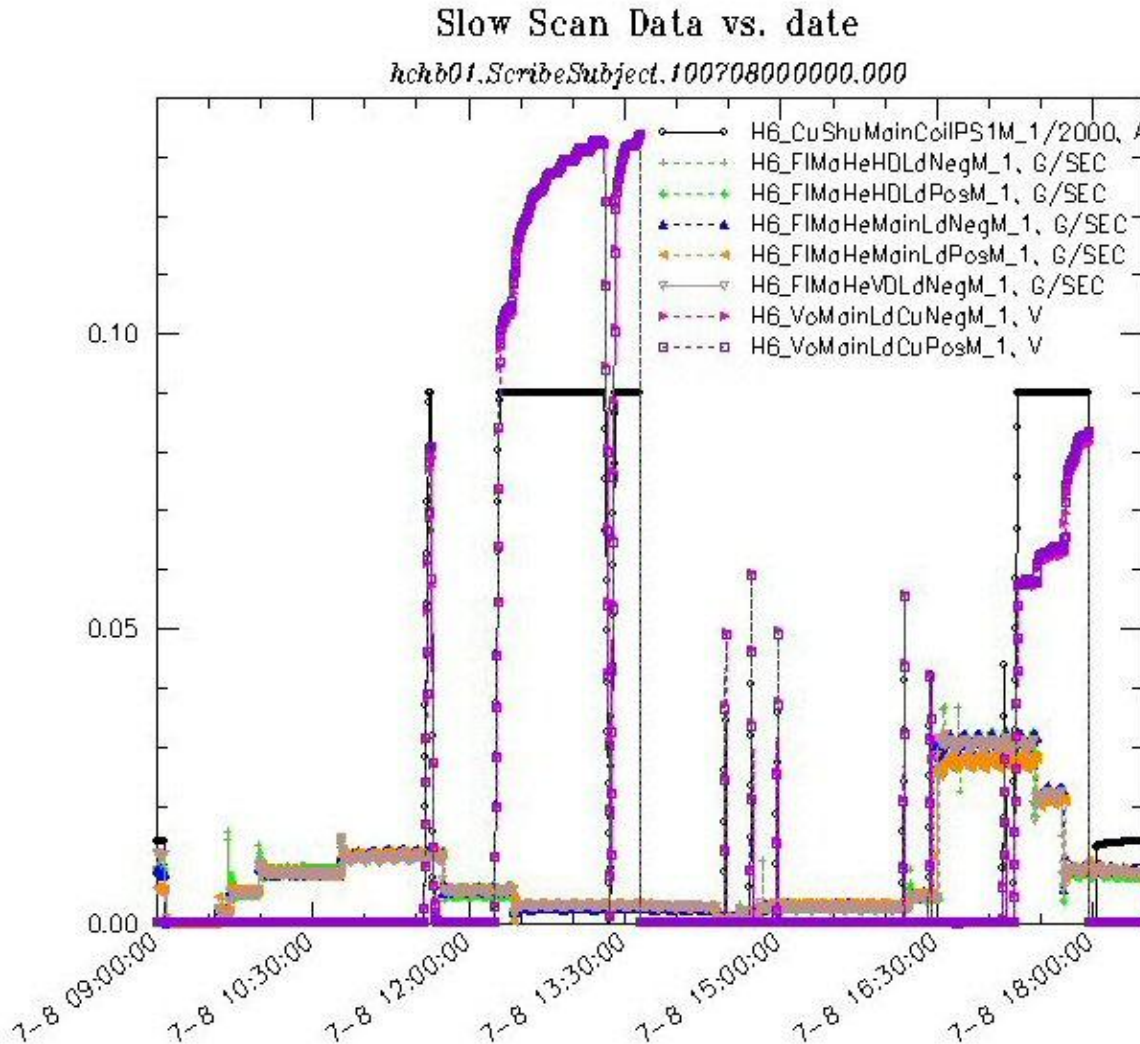


Fig. 12. Lead flows, solenoid current, and lead voltage history in continued lead flow study.

At this flow the magnet was ramped successfully to 180 A at 1 A/s and ran briefly with stable lead voltages, until a system trip occurred. Another ramp was then made at the lower flow of 2 sl/m (0.006 g/s), and lead voltages stabilized just above 0.1 V. The flows were lowered again to 1 sl/m and ran for an hour at 180 A with voltages approaching 0.135 V; the power supply profile then ramped down and up again, which showed that the lens could run at operating current, and ramp at 1 A/s without a quench, at this low flow rate! The 1/e time constant for voltages to stabilize is about 15 minutes.

However, because the lead voltages were slowly rising, the quench detection system tripped when total lead voltage reached threshold (the “current balance” factor had not been readjusted for changed flow conditions). Since this low lead flow rate had been successful, even lower rates were then tried; however, on each of 5 subsequent attempts – each with increased flow, up to 1.7 sl/m (0.005 g/s) which had previously worked - the solenoid coil quenched at 83.9 A. We came to the conclusion that heat must have been generated (by eddy currents) during the high-current trip, was trapped within the coil or vessel, and could only be removed quickly by increasing the lead flow rate. Therefore all flows were raised to 10.7 sl/m (0.030 g/s) for about 30 minutes, after which a ramp to 180 A was successful. Finally flows were sequentially lowered, to 7.5, then 3.0 sl/m, and each time voltages were allowed to stabilize.

Both leads performed identically, and Fig. 14 shows the asymptotic lead voltage versus helium lead flow (per lead, for all 6 leads) while operating at 180 A. Future tests will be made to explore the behavior at different currents, assuming it may be necessary to operate the lenses with some variation in focal length.

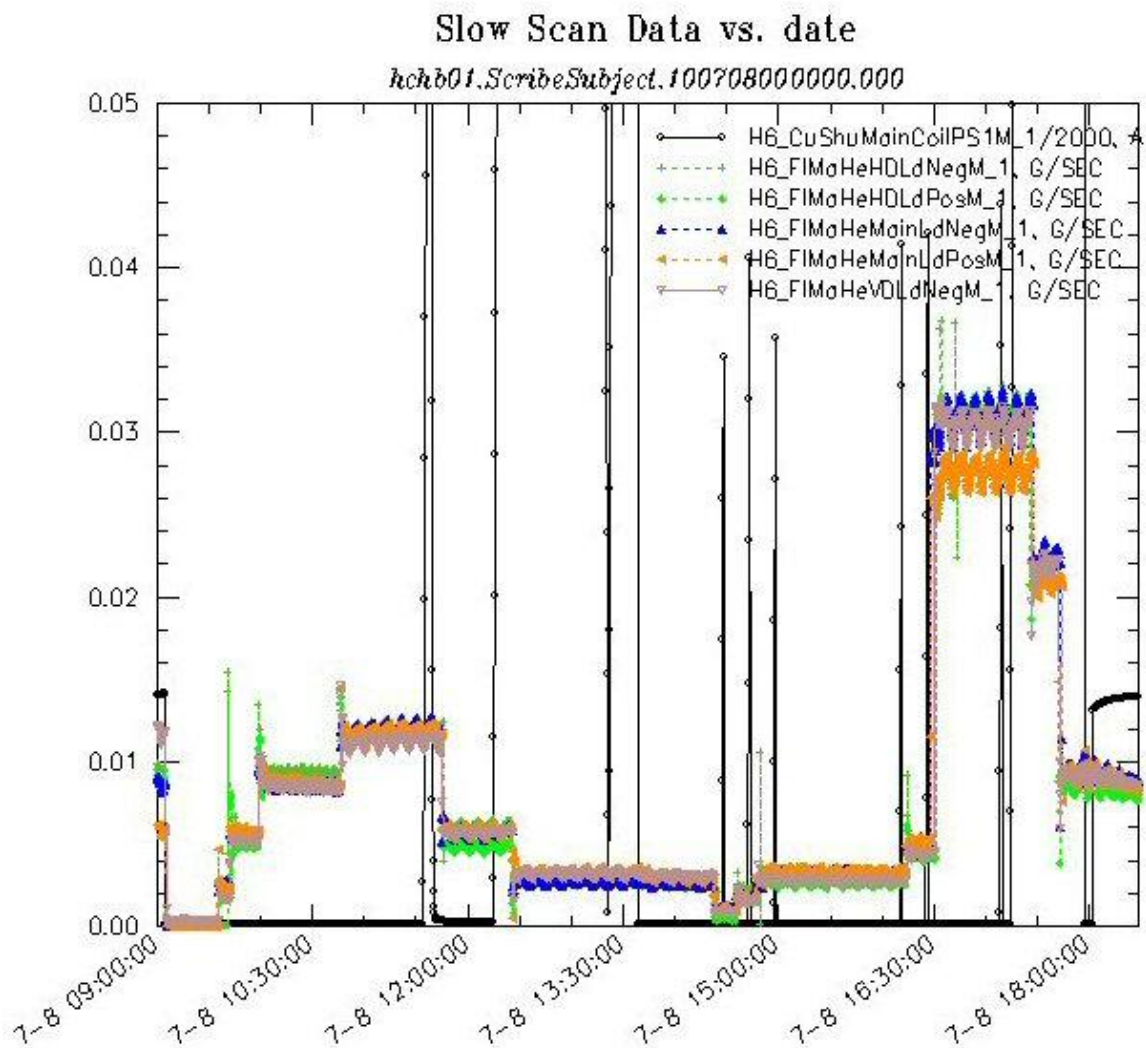


Fig. 13. Magnified view of lead flow history in continued lead flow study.

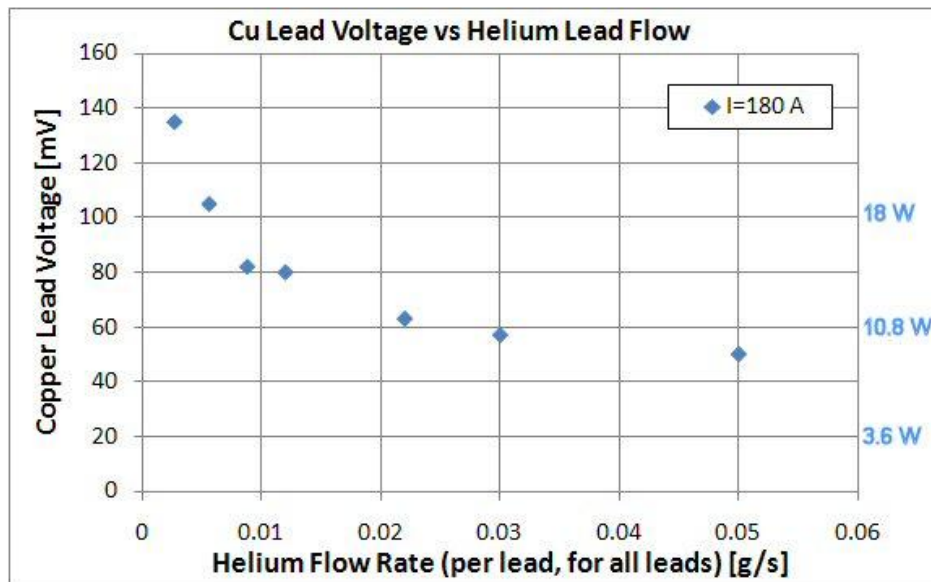


Fig. 14. Lead voltage (and dissipated power) versus lead flow at the nominal operating current.

### Solenoid Alignment

As with the prototype cryostatted solenoid [2], alignment measurements were made using Single Stretched Wire (SSW) techniques. Figure 15 shows the setup of the wire positioning stages, which allow wire positioning control at the level of 1 micron. In testing the prototype, the solenoid center and axis orientations were established using co- and counter- directional motions of the stages in a standard Moving Wire (MW) approach. A Vibrating Wire (VW) technique [6] was also developed and tested on the prototype, and was compared to the Moving Wire (MW) method. The VW position detection system is shown in Fig. 16. The VW gives more accurate results, chiefly because it is able to reduce systematic errors caused by the proximity of the stages to the magnet ends. The ends have relatively large fringe fields in the vicinity of the stage surfaces ( $\sim 50\text{G}$  at operating current) where the return wire is attached. The return wire therefore cuts flux lines during measurements when it rather needs to be stationary throughout the field of the magnet. The VW approach has no such complication since the mechanical vibrations are measured only on the stretched wire itself.

Furthermore, in principle, the VW can be operated at various frequencies to excite multiple oscillation modes, thereby giving some ability to explore the axial ( $Z$ ) dependence of the center – whose position may vary at the  $\leq 250$  micron level due to bucking and main coil offsets during fabrication. This extended capability has not yet been explored for these magnets.



Fig. 15. Single Stretched Wire alignment setup with cryostat assembly on MTF test stand 6.

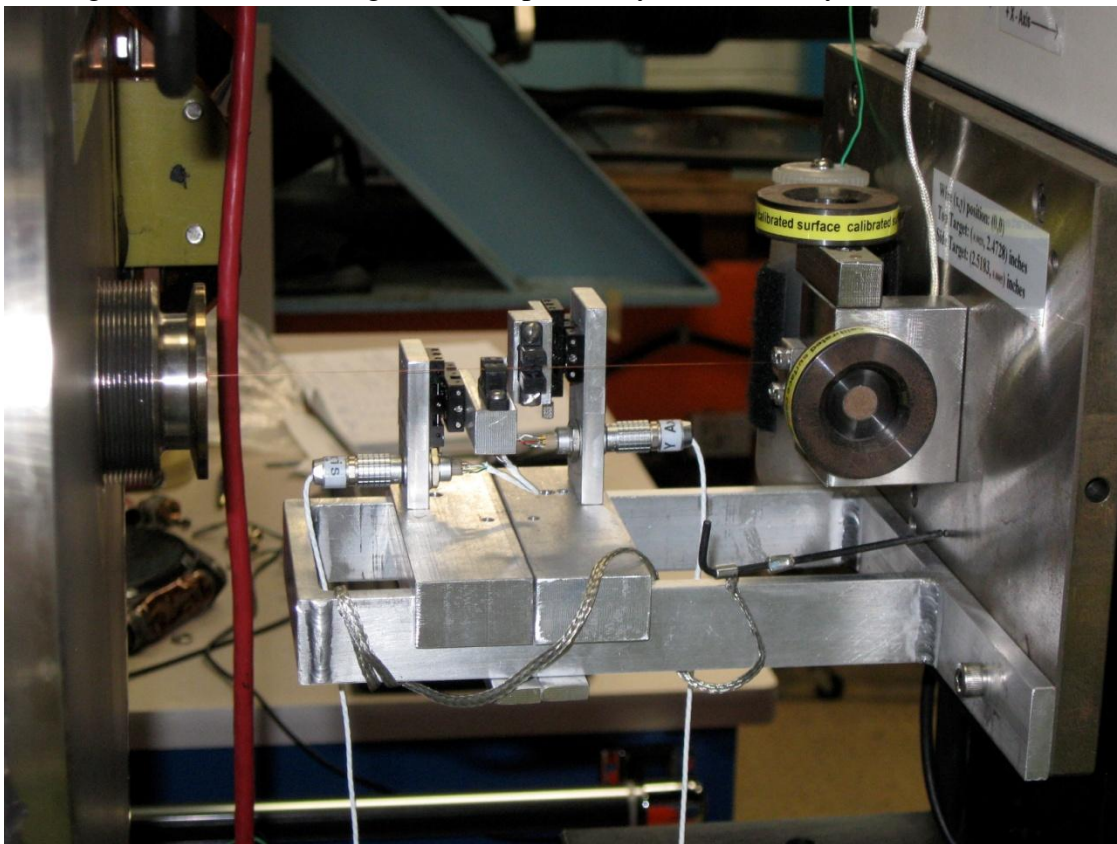


Fig. 16. Close-up of vibrating wire motion sensors.

Table 1 lists the sequence of solenoid axis and dipole field measurements. The results of alignment measurements during the various thermal cycles are shown in Figures 17 and 18, relative to the axis position during the first cold test (chosen as the zero axis). Note that the axis has been projected to points at  $Z = \pm 105\text{mm}$  (corresponding roughly to the axial ends of the cryostat) to indicate the pitch/yaw present. In this survey reference frame, the Y is vertical with positive coordinates up, X is horizontal with positive coordinates to the West, and Z is along the beam axis with positive coordinates to the South (away from the interface box); which is a left-handed system.

Table 1. Time table of warm and cold Alignment and Survey measurements.

Activity	Date VW alignment	Date Survey	Date Cryo Change
1 <sup>st</sup> Warm Measurement	5/4/2010	5/4/2010	
1 <sup>st</sup> Cool Down to 4.5K			5/22
1 <sup>st</sup> Cold Measurement	6/9	6/9	
Warm up to 300 K			6/17
2 <sup>nd</sup> Warm Measurement	6/22	6/22	
2 <sup>nd</sup> Cool Down to 4.5K			6/23
2 <sup>nd</sup> Cold Measurement	6/24	6/28	
Warm up to 300 K			7/9-14
3 <sup>rd</sup> Warm Measurement	7/21	7/21	

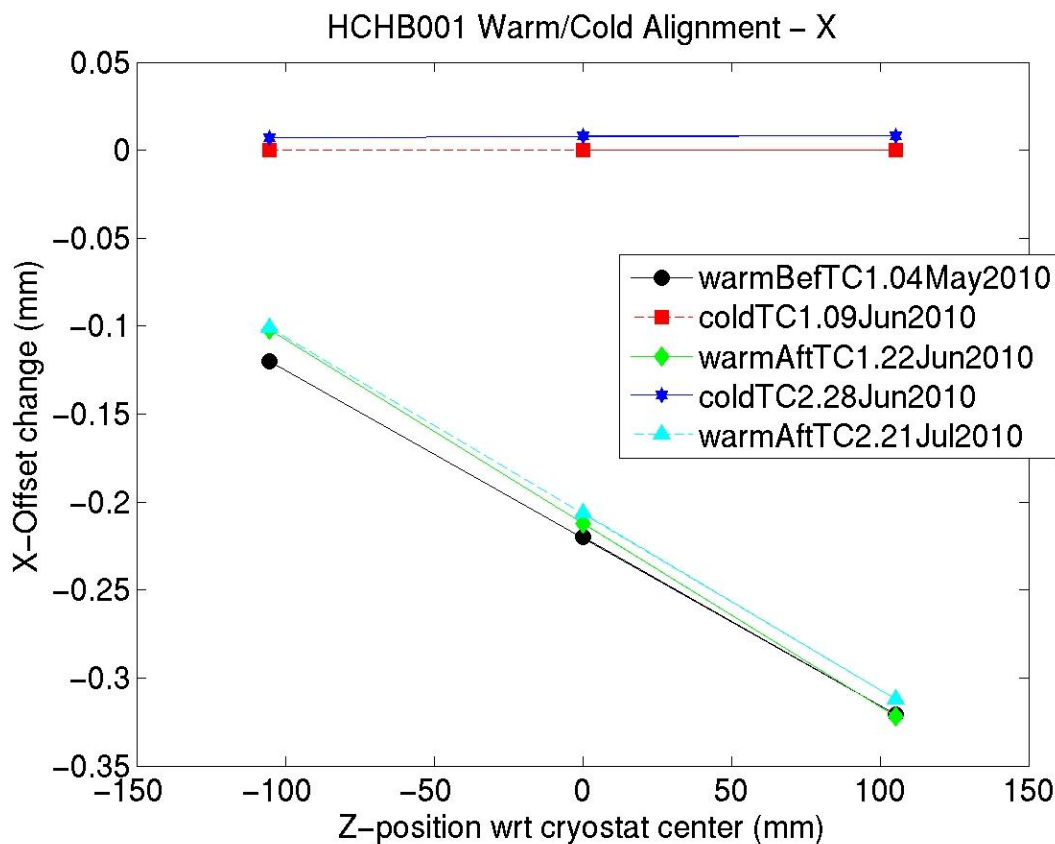


Figure 17. Summary of horizontal axis position of solenoid during cold/warm conditions relative to the alignment made at 4.4K during the first test cycle.

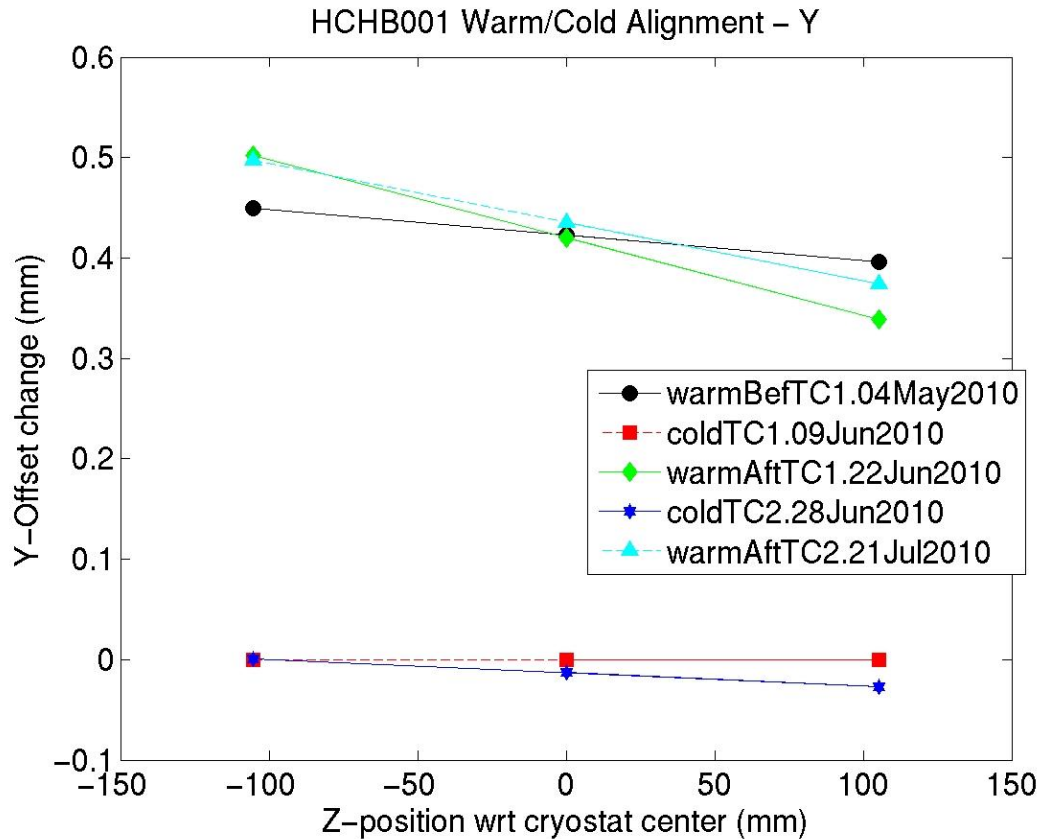


Figure 18. Summary of vertical axis position of solenoid during cold/warm conditions relative to the alignment made at 4.4K during the first test cycle.

Measurements taken to determine whether there was a dependence on the XY center offset vs. magnet current showed no measureable result – the center appears to be stable at the resolution of the measurements (< 10 microns).

A Hall Probe axis determination experiment is planned for a future thermal cycle. This technique was explored [7] during a qualification test of the final Type-1 production CH solenoid, and based upon those results a number of improvements have been made to the apparatus. The goal of this measurement is to explore the variation of magnet center along the solenoid axis, due to possible misalignments of the main and bucking coils.

### Steering Dipole Alignment

The steering dipoles were measured both warm and cold during the first test cycle. The roll angles were determined relative to gravity in the orientation that the magnet was mounted on the test stand. Survey results have not yet been transformed to reflect an optimization of this roll angle for mounting the magnets in the beam line. Warm data were taken with 12A AC current, and the results are summarized in Table 2.

Table 2. Results of warm steering dipole measurements

Corrector type	Field direction	Strength TF (T-m/kA)	Roll angle (mrad)	Angle s.d. (mrad)
Horizontal	vertical	0.0489	-12.83	0.17
Vertical	horizontal	0.0467	4.97	0.02

The measurement of the corrector during cold conditions was complicated by the presence of magnetization effects in the superconductor, which significantly impacts the results. Another difficulty is the signal size itself. With transfer function of  $\sim 0.05\text{T-m/kA}$ , even at 200A (0.2kA) excitation, the integrated field is  $\sim 10\text{mT-m}$ . With the small aperture, wire motion is restricted to roughly  $\pm 8\text{mm}$  which yields an integrated flux of about  $80\mu\text{V-s}$ . Since good noise levels for DC measurements are at the level of  $0.2\mu\text{V-s}$ , the expected resolution for angular measurements is on the order of 2.5 mrad. This limitation is reflected in the standard deviation (s.d.) values.

A summary of the cold data acquired for the dipole correctors is shown in Table 3. The strength TF and angle of the horizontal corrector as a function of current is shown in Figures 19 and 20 and indicate a large hysteresis. Note also that the vertical corrector roll angles measured at 50 and 200A changed dramatically after the horizontal corrector was powered. It is difficult to draw conclusions from the data taken to date. Further studies are required to better understand the dipole correctors and how they might perform when used as planned for the beam line.

Table 3. Results of cold steering dipole measurements (in sequence of measurements)

Cor.	Nom. Current (A)	Nmeas	Strength TF (T-m/kA)	Roll angle(mrad)	Ang. s.d. (mrad)
V	50	5	0.0384	14.3	14.5
V	200	10	0.0438	8.9	2.0
H	50	10	0.0442	235.7	11.9
H	200	10	0.0461	30.2	2.2
H	120	3	0.0486	54.7	5.1
H	160	3	0.0468	39.4	2.4
H	80	2	0.0506	84.8	0.1
H	50	2	0.0535	129.8	7.0
H	120	1	0.0469	52.5	-
H	200	1	0.0463	23.9	-
V	50	5	0.0467	212.2	9.4
V	120	1	0.0434	86.2	-
V	200	1	0.0434	44.0	-

To try to quantify the size of effects, we note that the change in angle of the vertical corrector at 200A before and after powering the horizontal is about 30 mrad, or about 0.03 of the strength TF. This implies a change in the orthogonal field (presumably stemming from a remnant field in the horizontal corrector) equivalent to about 6A ( $0.03 * 200\text{A}$ ).

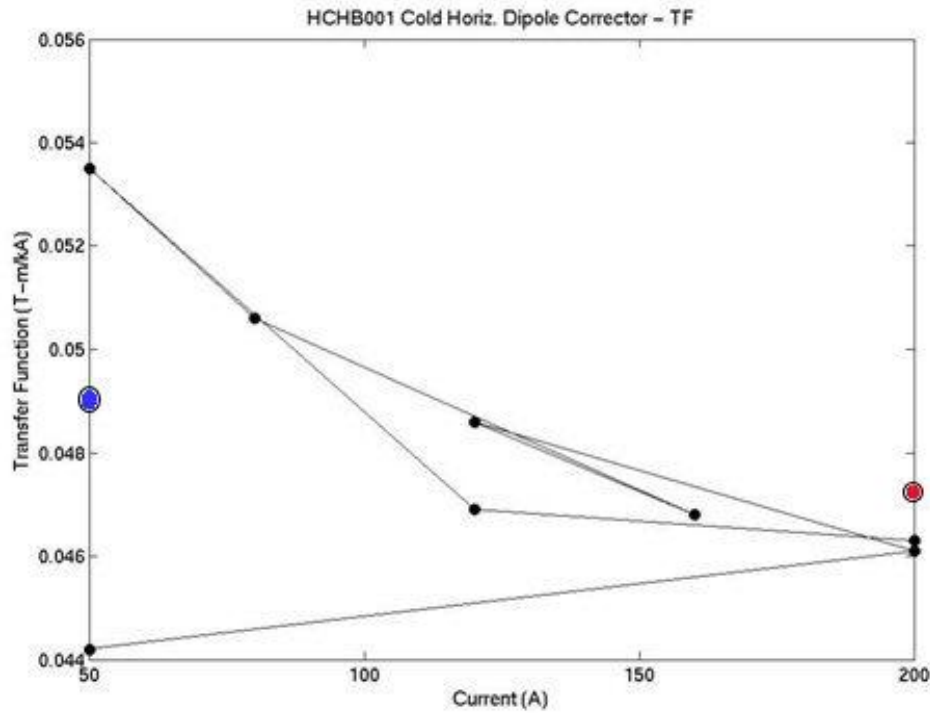


Figure 19. Transfer Function of horizontal steering dipole measured as a function of current. The sequence of measurements is that listed in Table 3. The TF measured with Hall probe scan at 200 A is superimposed as a red point, the warm TF (12 A, AC) is shown as a blue point.

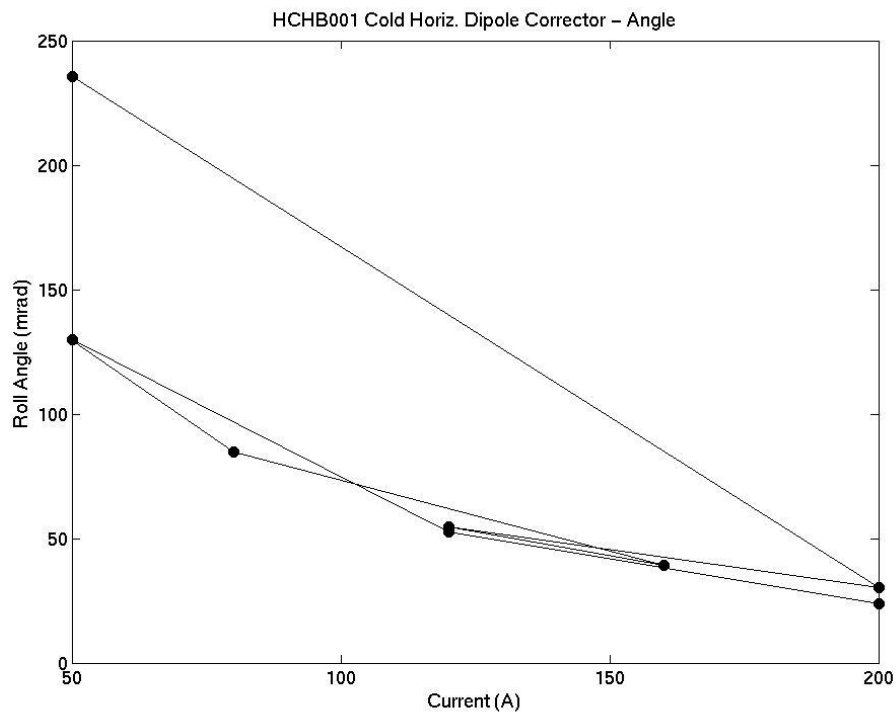


Figure 20. Roll angle of horiz. steering dipole measured as a function of current from Table 3.

## Conclusions

A first set of quench, thermal, and alignment performance tests has been completed on the first production Type-2 cryostatted solenoid focusing lens for the HINS R&D proton linac. The lens has performed reasonably well but there are some issues that require more study in all of these areas. Therefore a supplemental test plan has been drawn up to establish the optimal operating parameters for use in the beam line, and to further explore the performance under conditions other than the nominal operating point.

## REFERENCES

- [1] T. M. Page, et al., "HINS Superconducting Lens and Cryostat Performance", *IEEE Trans. Appl. Supercond.*, No. 19, pp1356-1359, 2009.
- [2] T. Page, et al., "High intensity neutrino source superconducting solenoid cryostat design," AIP Conf. Proc. Vol. 985, pp341-348, March 2008.
- [3] D. Orris, M. Tartaglia, "Superconducting Strand Quench Development Tests," Technical Division Note TD-09-012, FNAL, April 2009.
- [4] G. Davis, et al., "HINS\_CH\_SOL\_03d-1 Fabrication Summary and Test Results," Technical Division Note TD-08-002, FNAL, January 2008.
- [5] G. Davis, et al., "HINS\_CH\_SOL\_06 Fabrication and Test Results," Technical Division Note TD-08-004, FNAL, January 2008.
- [6] A. Temnykh, "Vibrating Wire Field-measuring Technique", *Nuclear Instruments and Methods in Physics Research A* 399 (1997), 185-194.
- [7] M. Tartaglia, C. Hess, "A Study of HINS CH Solenoid Axis Determination with Hall Probe Measurements," Technical Division Note TD-10-017, FNAL, August 2010.